Inorg. Chem. **2006**, *45*, 4423–4430

Self-Assembly, Structures, and Solution Dynamics of Emissive Silver Metallacycles and Helices

Ronger Lin and John H. K. Yip*

Department of Chemistry, National University of Singapore, 3 Science Drive 3, Singapore, 11754, Singapore

Received January 24, 2006

Reactions of 9,10-bis(diphenylphosphino)anthracene (PAnP) and AgX (X = OTf^-, ClO_4^-, PF_6^-, and BF_4^-) led to luminescent Ag–PAnP complexes with rich structural diversity. Helical polymers $[Ag(\mu\text{-PAnP})(CH_3CN)X]_n$ (X = OTf^-, ClO_4^-, and PF_6^-) and discrete binuclear $[Ag_2(\mu\text{-PAnP})_2(CH_3CN)_4](PF_6)_2$, trinuclear $[Ag_3(\mu\text{-PAnP})_3\supset BF_4](BF_4)_2$, and tetranuclear $[Ag_4(\mu\text{-PAnP})_4\supset(ClO_4)_2](ClO_4)_2$ metallacycles were isolated from different solvents. The tri- and tetranuclear metallacycles exhibited novel puckered-ring and saddlelike structures. Variable-temperature (VT) $^{31}P\{^1H\}$-NMR spectroscopy of the complexes was solvent dependent. The dynamics in CD_3CN involve two species, but the exchange processes in CD_2Cl_2 are more complicated. A ring-opening polymerization was proposed for the exchange mechanism in CD_3CN.

Introduction

Metal directed self-assembly is an effective approach toward coordination polymers and metallacycles.[1] Supramolecular assemblies arising from silver-ligand coordination are known for their complexity and rich structural diversity.[2] Many studies showed that combinations of a Ag^I ion and multidentate ligands often give rise to more than one product, which could be polymer or discrete metallacycles. It is due to the various coordination geometry possibly adopted by the Ag^I ion[3] and the labile Ag-ligand bond which results in equilibrium of different species in solution. The position of the equilibrium could be influenced by factors such as temperature, solvent, and anion, making the self-assembly less predictable and controllable.[4,5]

Most works on silver-ligand self-assembly invoke N-heterocyclic ligands.[1a,2−6] As an important class of ligands for late transition metals, phosphines have been recently used in constructing metallo-supramolecular systems.[7−10] A number of Ag−diphosphine supramolecules have been reported. Noteworthy is the work of Puddephatt which showed that

* To whom correspondence should be addressed. E-mail: chmyiphk@nus.edu.sg. Fax: 65-67791691.

(1) For reviews see (a) Khlobystov, A. N.; Blake, A. J.; Champness, N. R.; Lemenovskii, D. A.; Majouga, A. G.; Zyk, N. V.; Schröder, M. *Coord. Chem. Rev.* **2001**, *222*, 155. (b) Leininger, S.; Olenyuk, B.; Stang, P. J. *Chem. Rev.* **2000**, *100*, 853. (c) Batten, S. R.; Robson, R. *Angew. Chem., Int. Ed.* **1998**, *37*, 1461.

(2) (a) Dong, Y.-B.; Zhang, H.-Q.; Ma, J.-P.; Huang, R.-Q.; Su, C.-Y. *Cryst. Growth Des*. **2005**, *5*, 1857. (b) Withersby, M. A.; Blake, A. J.; Champness, N. R.; Hubberstey, P.; Li, W.-S. Schröder, M. *Angew. Chem., Int. Ed. Engl.* **1997**, *36*, 2327. (c) Blake, A. J.; Baum, G.; Champness, N. R.; Chung, S. S.-M.; Cooke, P. A.; Fenske, D.; Khlobystov, A. N.; Lemenovskii, D. A.; Li, W.-S.; Schröder, M. *J. Chem. Soc., Dalton Trans.* **2000**, 4285. (f) Muthu, S.; Yip, J. H. K.; Vittal, J. J. *J. Chem. Soc., Dalton Trans.* **2002**, 4561. (g) Muthu, S.; Yip, J. H. K.; Vittal, J. J. *J. Chem. Soc., Dalton Trans.* **2001**, 3577.

(3) (a) Venkataraman, D.; Du, Y.; Wilson, S. R.; Hirsch, K. A.; Zhang, P.; Moore, J. S. *J. Chem. Edu.* **1997**, *74*, 915. (b) Cotton, F. A.; Wilkinson, G. *Advanced Inorganic Chemistry*, 5th ed.; Wiley: Chichester, **1988**.

(4) Blake, A. J.; Champness, N. R.; Cooke, P. A.; Nicolson, J. E. P.; Wilson, C. *J. Chem. Soc., Dalton Trans.* **2000**, 3811.

(5) Hannon, M. J.; Painting, C. L.; Plummer, E. A.; Childs, L. J.; Alcock, M. W. *Chem.—Eur. J.* **2002**, 2225.

(6) (a) Chen, C.-L.; Su, C.-Y.; Cai, Y.-P.; Zhang, H.-X.; Xu, A.-W.; Kang, B.-S.; zur Loye, H.-C. *Inorg. Chem.* **2003**, *42*, 3738. (b) Su, C.-Y.; Cai, Y.-P.; Chen, C.-L.; Smith, M. D.; Kaim, W.; zur Loye, H.-C. *J. Am. Chem. Soc.* **2003**, *125*, 8595. (c) Bray, D. J.; Liao, L. L.; Antonioli, B.; Gloe, K.; Lindoy, L. F.; McMurtrie, J. C.; Wei, G.; Zhang, X.-Y. *J. Chem. Soc., Dalton Trans.* **2005**, 2082. (d) Burchell, T. J.; Eisler, D. J.; Puddephatt, R. J. *J. Chem. Soc. Chem. Comm.* **2004**, 944. (e) Yue N. L. S.; Jennings, M. C.; Puddephatt, R. J. *Inorg. Chem.* **2005**, *44*, 1125. (f) Yue, N. L. S.; Jennings, M. C.; Puddephatt, R. J. *J. Chem. Soc., Chem. Commun.* **2005**, 4792.

(7) (a) Eisler, D. J.; Puddephatt, R. J. *Inorg. Chem.* **2003**, *42*, 8192. (b) Brandys, M. C.; Puddephatt, R. J. *J. Am. Chem. Soc.* **2002**, *124*, 3946. (c) Eisler, D. J.; Puddephatt, R. J. *Cryst. Growth Des.* **2005**, *5*, 57.

(8) (a) James, S. J. *Macromol. Symp.* **2004**, *209*, 119. (b) James, S. L.; Xu, X. L.; Law, R. V. *Macromol. Symp.* **2003**, *196*, 187. (c) Lozano, E.; Nieuwenhuyzen, M.; James, S. L. *Chem.—Eur. J.* **2001**, *7*, 2644. (d) Miller, P.; Nieuwenhuyzen, M.; Charmant, J. P. H.; James, S. L. *CrystEngComm* **2004**, *6*, 408. (e) James, S. L.; Lozano, E.; Nieuwenhuyzen, M. *J. Chem. Soc., Chem. Commun.* **2000**, 617.

(9) (a) Lu X.-L.; Leong W. K.; Hor T. S. A.; Goh L. Y. *J. Organomet. Chem.* **2004**, 689, 1746. (b) Lu, X.-L.; Leong, W. K.; Goh, L. Y.; Hor, T. S. A. *Eur. J. Inorg. Chem.* **2004**, 2504.

(10) (a) Bessel, C. A.; Aggarwal, P.; Marschilok, A. C.; Takeuchi, K. J. *Chem. Rev.* **2001**, *101*, 1031. (b) Caruso, F.; Camalli, M.; Rimml, H.; Venanzi, L. M. *Inorg. Chem.* **1995**, *34*, 673. (c) Kitagawa, S.; Kondo, M.; Kawata, S.; Wada, S.; Maekawa, M.; Munataka, M. *Inorg. Chem.* **1995**, *34*, 1455. (d) Bachechi, F.; Burini, A.; Galassi, R.; Pietroni, B. R.; Jesei, D. *Eur. J. Inorg. Chem.* **2002**, 2086.

10.1021/ic060140v CCC: $33.50
Published on Web 05/06/2006

Scheme 1. Reactions of PAnP and AgX (X = OTf−, ClO_4−, PF_6−, and BF_4−)

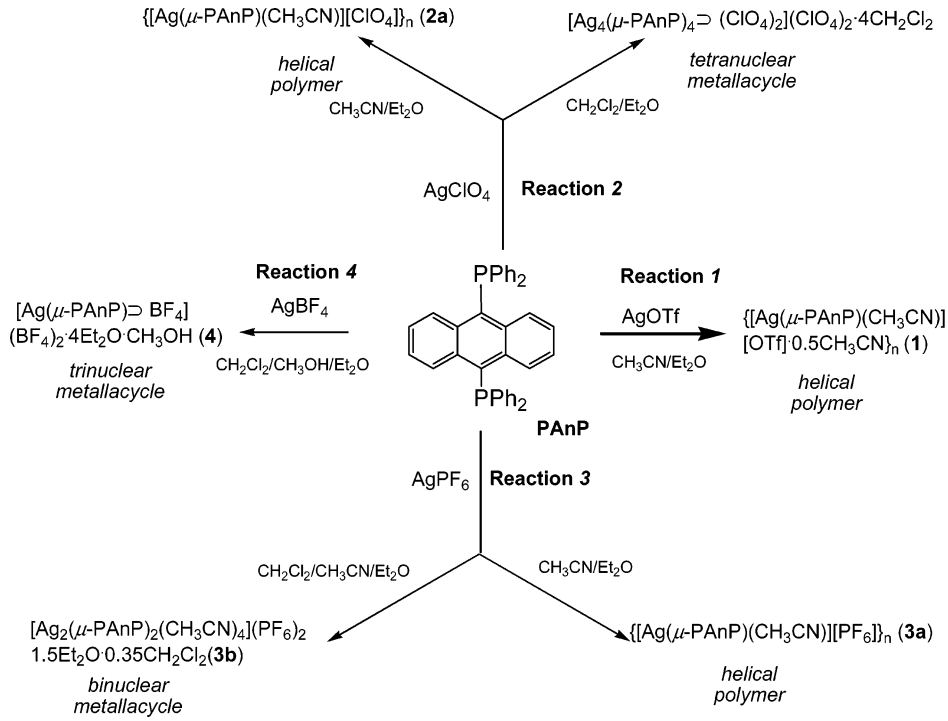

changing the rigidity of the backbone of the diphosphine ligand could have drastic effect on the outcome of the self-assembly.[7b] The Ag−phosphine supramolecules usually display complex solution dynamics.[8a,b]

Described in this paper are reactions of 9,10-bis(diphenylphosphino)anthracene (PAnP) (Scheme 1) and various AgX (AgX, X = OTf^-, PF_6^-, BF_4^-, and ClO_4^-) and structures and solution dynamics of the products. PAnP, first synthesized by our group, has been shown to form stable gold(I)-metallacycles.[11,12] The ligand has two special features: First, with the chromophoric anthracenyl ring in its backbone, the ligand is capable of imparting luminescence to its metal complexes.[11,12] Second, the anthracenyl backbone can participate in $\pi-\pi$ stacking and C−H···π interactions, which could lead to new supramolecular architectures.[12,13] Our present study showed that reactions of Ag^I ion and the ligand gave rise to discrete metallacycles and helical polymers which exhibited complicated dynamics in solution.

Experimental Section

General Methods and Physical Measurements. Compound 9,10-bis(diphenylphosphino)anthracene (PAnP) was synthesized according to the reported method.[12] All silver salts were purchased from Aldrich and used without being purified. The UV−vis absorption and emission spectra of the complexes were recorded on a Shimadzu UV-1601 UV−visible spectrophotometer and a Perkin-Elmer LS-50B fluorescence spectrophotometer, respectively. Electrospray ionization mass spectra (ESI-MS) were measured on a Finnigan MAT 731 LCQ spectrometer. Elemental analyses of the complexes were carried out at the National University of Singapore, Singapore.

Synthesis of $\{[Ag(\mu\text{-PAnP})(CH_3CN)(OTf)]\cdot 0.5CH_3CN\}_n$ (1). A 5 mL CH_3CN solution of AgOTf (52 mg, 0.20 mmol) was added into a 50 mL CH_2Cl_2 solution of PAnP (110 mg, 0.20 mmol) under N_2. The mixture was stirred for 2 h in the dark. The addition of Et_2O to the concentrated solution precipitated yellow solids. Yield: 73%. Crystals were obtained from CH_3CN/Et_2O. Anal. Calcd for $C_{42}H_{32.5}AgF_3N_{1.5}O_3P_2S$: C, 58.31%; H, 3.79%. Found: C, 57.89%; H, 3.49%. $^{31}P\{^1H\}$-NMR: see text. ^1H NMR (CD_3CN, 300 MHz): δ 7.91−7.87 (m, 4H), 7.52−7.25 (m, 20H), 6.86−6.82 (m, 4H). ESI-MS (*m*/*z* assignment): 654.3, $[Ag(PAnP)]_n^{n+}$; 926.9, $[Ag_2(PAnP)_3]^{2+}$; 1201.0, $[Ag(PAnP)_2]^+$; 1745.4, $[Ag(PAnP)_3]^+$.

Synthesis of $\{[Ag(\mu\text{-PAnP})(CH_3CN)(ClO_4)]\}_n$ (2a) and $[Ag_4(\mu\text{-PAnP})_4\supset(ClO_4)_2](ClO_4)_2\cdot 4CH_2Cl_2$ (2b). The preparation of complex **2a** was similar to that of complex **1**. Yield: 77%. Compound **2a** $\{[Ag(\mu\text{-PAnP})(CH_3CN)][ClO_4]\}_n$ was crystallized from a CH_3CN/Et_2O solution of the product obtained from the reaction of $AgClO_4$ and PAnP. Anal. Calcd for $C_{80}H_{62}Ag_2Cl_2N_2O_8P_4$: C, 60.44%; H, 3.93%. Found: C, 59.52%; H, 3.74%. $^{31}P\{^1H\}$-NMR: see text. ^1H NMR (CD_3CN, 300 MHz): δ 7.91−7.88 (m, 4H), 7.52−7.24 (m, 20H), 6.86−6.82 (m, 4H). ESI-MS (*m*/*z* assignment): 654.3, $[Ag(PAnP)]_n^{n+}$; 835.3, $[Ag_3(PAnP)_4]^{3+}$; 926.9, $[Ag_2(PAnP)_3]^{2+}$; 1201.0, $[Ag(PAnP)_2]^+$. Compound **2b** $[Ag_4(\mu\text{-PAnP})_4\supset(ClO_4)_2](ClO_4)_2\cdot 4CH_2Cl_2$ was obtained from the crystallization of CH_2Cl_2/Et_2O solution of the product obtained from the reaction of $AgClO_4$ and PAnP. Anal. Calcd for $C_{156}H_{120}Ag_4Cl_{12}O_{16}P_8$: C, 55.84%; H, 3.60%. Found: C, 55.43%; H, 3.51%. $^{31}P\{^1H\}$-NMR: see text. ^1H NMR (CD_2Cl_2, 300 MHz): δ 7.91−7.88 (m, 4H), 7.52−7.25 (m, 20H), 6.85−6.82 (m, 4H). ESI-MS (*m*/*z* assignment): 654.3, $[Ag(PAnP)]_n^{n+}$; 1031.0 $[Ag_3(PAnP)_3(ClO_4)]^{2+}$; 926.9, $[Ag_2(PAnP)_3]^{2+}$; 1201.0, $[Ag(PAnP)_2]^+$; 1408.6, $[Ag_2(PAnP)_2(ClO_4)]^+$ or $[Ag_4(PAnP)_4(ClO_4)_2]^{2+}$.

Synthesis of $\{[Ag(\mu\text{-PAnP})(CH_3CN)(PF_6)\}_n$ (3a) and $[Ag_2(\mu\text{-PAnP})_2(CH_3CN)_4](PF_6)_2\cdot 1.5Et_2O\cdot 0.35CH_2Cl_2$ (3b). Similar to the

(11) Yip, J. H. K.; Prabhavathy, J. *Angew. Chem., Int. Ed*. **2001**, *40*, 2159.
(12) Lin, R.; Yip, J. H. K.; Zhang, K.; Koh, L. L.; Wong, K.-Y.; Ho, K. P. *J. Am. Chem. Soc*. **2004**, *126*, 15852.
(13) Zhang, K.; Prabhavathy, J.; Yip, J. H. K.; Koh, L. L.; Tan, G. K.; Vittal, J. J. *J. Am. Chem. Soc.* **2003**, *125*, 8452.

Table 1. Crystal Data and Structure Refinements[a] for Compounds **1**, **2a**, **2b**, **3a**, **3b**, and **4**

	1	**2a**	**2b**	**3a**	**3b**	**4**
empirical formula	$C_{42}H_{32.50}AgF_3N_{1.50}O_3P_2S$	$C_{80}H_{62}Ag_2Cl_2N_2O_8P_4$	$C_{156}H_{120}Ag_4C_{112}O_{16}P_8$	$C_{80}H_{62}Ag_2F_{12}N_2P_6$	$C_{90.45}H_{83.90}Ag_2Cl_{0.70}F_{12}N_4O_{1.50}P_6$	$C_{131}H_{127}Ag_3B_3F_{12}O_5P_6$
fw	865.07	1589.84	3355.16	1680.88	1905.29	2551.19
T (K)	223(2)	223(2)	223(2)	223(2)	293(2)	223(2)
cryst syst	monoclinic	orthorhombic	orthorhombic	orthorhombic	orthorhombic	monoclinic
space group	$P2(1)/c$	$P2(1)2(1)2(1)$	$Fddd$	$P2(1)2(1)2(1)$	$Pmn2(1)$	Cc
a (Å)	14.092(2)	9.7009(6)	19.4287(7)	9.7572(5)	18.7319(8)	15.7878(14)
b (Å)	9.7574(15)	14.5954(10)	36.4741(12)	14.8314(8)	18.5100(8)	39.138(4)
c (Å)	29.812(5)	24.0063(16)	42.9932(15)	24.1685(14)	25.8368(11)	21.1625(17)
α (deg)	90	90	90	90	90	90
β (deg)	101.907(4)	90	90	90	90	111.148(2)
γ (deg)	90	90	90	90	90	90
V (Å^3)	4011.0(11)	3399.0(4)	30466.9(18)	3497.5(3)	8958.3(7)	12195.7(19)
Z	4	2	8	2	4	4
D_{calcd} (g/cm^3)	1.433	1.553	1.463	1.596	1.413	1.389
abs coeff (mm^{-1})	0.688	0.810	0.862	0.777	0.638	0.627
F(000)	1756	1616	13568	1696	3882	5228
total no. of reflns	22 737	23 875	43 028	20 514	51 160	17 538
independent reflns	7077 [$R_{(int)}$ = 0.0667]	7791 [$R_{(int)}$ = 0.0432]	6714 [$R_{(int)}$ = 0.0925]	6151 [$R_{(int)}$ = 0.0433]	16104 [$R_{(int)}$ = 0.0280]	17538 [$R_{(int)}$ = 0.0609]
no. of params varied	477	433	462	461	1106	1181
index ranges	$-16 \le h \le 16$, $-11 \le k \le 11$, $-33 \le l \le 33$	$-11 \le h \le 12$, $-18 \le k \le 18$, $-31 \le l \le 28$	$-20 \le h \le 23$, $-40 \le k \le 43$, $-51 \le l \le 51$	$-11 \le h \le 11$, $-17 \le k \le 17$, $-19 \le l \le 28$	$-22 \le h \le 19$, $-22 \le k \le 21$, $-30 \le l \le 30$	$-18 \le h \le 18$, $-46 \le k \le 45$, $-25 \le l \le 19$
2θ range for data collection (deg)	2.96−50.00	3.26−55.00	3.70−50.00	3.22−50.00	4.34−50.00	2.94−50.00
largest difference peak and hole (e·Å^{-3})	2.196 and −0.614	3.699 and −0.409	1.786 and −1.092	1.448 and −0.379	0.822 and −0.308	0.891 and −0.412
final R indices [$I > 2\sigma(I)$][b]	R1 = 0.0664, wR2 = 0.1698	R1 = 0.0708, wR2 = 0.1853	R1 = 0.0843, wR2 = 0.2108	R1 = 0.0520, wR2 = 0.1233	R1 = 0.0412, wR2 = 0.1158	R1 = 0.0660, wR2 = 0.1513
GOF[c] on F^2	0.954	1.054	1.087	1.148	1.061	0.966

[a] For all crystal determinations, scan type and wavelength of radiation used are ω and 0.71073 Å, respectively. [b] $R1 = (||F_o| - |F_c||)/(|F_o|)$; $wR2 = [w(F_o^2 - F_c^2)/w(F_o^4)]^{1/2}$. [c] $GOF = [(w(F_o^2 - F_c^2)^2/(n - p)]^{1/2}$.

other reactions of AgX and PAnP, the reaction of $AgPF_6$ and PAnP led to the formation of a yellow product. Yield: 70%. Compound **3a** $\{[Ag(\mu\text{-PAnP})(CH_3CN)][PF_6]\}_n$ was crystallized from a CH_3CN/Et_2O solution. Anal. Calcd for $C_{80}H_{62}Ag_2F_{12}N_2P_6$: C, 57.16%; H, 3.72%. Found: C, 56.44%; H, 3.39%. $^{31}P\{^1H\}$-NMR: see text. ^1H NMR (CD_3CN, 300 MHz): δ 7.91−7.88 (m, 4H), 7.52−7.25 (m, 20H), 6.85−6.82 (m, 4H). ESI-MS (*m*/*z*, assignment): 654.3, $[Ag(PAnP)]_n^{n+}$; 926.9, $[Ag_2(PAnP)_3]^{2+}$; 1201.0, $[Ag(PAnP)_2]^+$. Compound **3b** $[Ag_2(\mu\text{-PAnP})_2(CH_3CN)_4](PF_6)_2 \cdot 1.5Et_2O \cdot 0.35CH_2Cl_2$ was crystallized from a $CH_3CN/CH_2Cl_2/Et_2O$ solution of the product obtained from the reaction of $AgPF_6$ and PAnP. Anal. Calcd for $C_{90.45}H_{83.90}Ag_2Cl_{10.70}F_{12}N_4O_{1.5}P_6$: C, 48.07%; H, 3.74%. Found: C, 48.41%; H, 3.62%. $^{31}P\{^1H\}$-NMR: see text. ^1H NMR (CD_2Cl_2, 300 MHz): δ 7.96−7.93 (m, 4H), 7.62−7.38 (m, 20H), 6.68−6.65 (m, 4H). ESI-MS (*m*/*z*, assignment): 654.3, $[Ag(PAnP)]_n^{n+}$; 926.9, $[Ag_2(PAnP)_3]^{2+}$; 1201.0, $[Ag(PAnP)_2]^+$; 1054.3, $[Ag_2(PAnP)_2(PF_6)]^+$ or $[Ag_4(PAnP)_4(PF_6)_2]^{2+}$.

Synthesis of $[Ag_3(\mu\text{-PAnP})_3 \supset BF_4](BF_4)_2 \cdot 4Et_2O \cdot CH_3OH$ (4). The preparation of **4** was similar to that of **1** but with $AgBF_4$ (39 mg, 0.20 mmol) and PAnP (110 mg, 0.20 mmol). Yield: 87%. Anal. Calcd for $C_{131}H_{127}Ag_3B_3F_{12}O_5P_6$: C, 61.67%; H, 5.02%. Found: C, 59.73%; H, 4.13%. $^{31}P\{^1H\}$-NMR (CD_3CN, 121 MHz): δ 2.48 (br). $^{31}P\{^1H\}$-NMR: see text. ^{19}F NMR spectrum (CD_2Cl_2, 282 Hz): δ -84.3(s). ^1H NMR spectrum (CD_2Cl_2, 300 MHz): δ 7.92−7.89 (m, 4H), 7.52−7.22 (m, 20H), 6.86−6.83 (m, 4H). ESI-MS (*m*/*z*, assignment): 654.3, $[Ag(PAnP)]_n^{n+}$; 1025.1, $[Ag_3(PAnP)_3(BF_4)]^{2+}$; 926.9, $[Ag_2(PAnP)_3]^{2+}$; 1201.0, $[Ag(PAnP)_2]^+$; 1561, $[Ag_2(PAnP)_2(BF_4)]^+$ or $[Ag_4(PAnP)_4(BF_4)]^+$.

X-ray Crystallography. The diffraction experiments were carried out on a Bruker AXS SMART CCD three-circle diffractometer with a sealed tube at 23 °C using graphite-monochromated Mo Kα radiation (λ = 0.710 73 Å). The software used were SMART[14a] for collecting frames of data, indexing reflection, and determination of lattice parameters; SAINT[14a] for integration of intensity of reflections and scaling; SADABS[14b] for empirical absorption correction; and SHELXTL[14c] for space group determination, structure solution, and least-squares refinements on $[F]^2$. The crystals were mounted at the end of glass fibers and used for the diffraction experiments. Anisotropic thermal parameters were refined for the rest of the non-hydrogen atoms. The hydrogen atoms were placed in their ideal positions. A brief summary of crystal data and experimental details are given in Table 1.

Results and Discussion

Synthesis Reactions of AgX (X = OTf^-, PF_6^-, BF_4^-, and ClO_4^-) and PAnP, carried out in CH_3CN/CH_2Cl_2 at room temperature, resulted in clear yellow solutions from which bright yellow solids were isolated. In the following discussion, the reactions between PAnP and AgOTf, $AgClO_4$, $AgPF_6$, and $AgBF_4$ are referred to as reactions 1, 2, 3, and 4, respectively. Depending on the solvents used for crystallization, different complexes were isolated. Complexes **1a**, **2a**, and **3a** were crystallized from a CH_3CN/ether solution of the products of reactions 1, 2, and 3, respectively.

(14) (a) *SMART & SAINT Software Reference Manuals*, version 4.0; Siemens Energy & Automation, Inc., Analytical Instrumentation: Madison, WI, 1996. (b) Sheldrick, G. M. *SADABS: A Software for Empirical Absorption Correction;* University of Gottingen: Gottingen, Germany, 1996. (c) *SHELXTL Reference Manual*, version 5.03; Siemens Energy & Automation, Inc., Analytical Instrumentation: Madison, WI, 1996.

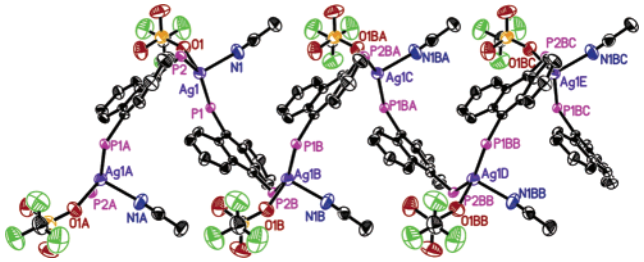

Figure 1. ORTEP plots of **1**: green, F; red, O; yellow, S. Hydrogen atoms, Ph rings, and solvent molecules are omitted. Thermal ellipsoids are drawn with 50% probability.

Table 2. Selected Bond Lengths (Å) and Angles (deg) for Complexes **1**, **2a**, and **3a**

	complex **1**	complex **2a**	complex **3a**
Ag(1)−N(1)	2.389(7)	2.393(7)	2.370(7)
Ag(1)−P(1)	2.4941(19)	2.4954(15)	2.4741(13)
Ag(1)−P(2)	2.4976(19)	2.5035(14)	2.4875(12)
Ag(1)−O(1)	2.519(5)	2.679(14)	
Ag(1)−F(6)			2.925(9)
P(1)−Ag(1)−P(2)	150.73(5)	148.71(5)	150.79(5)
C(1)−P(1)−Ag(1)	116.40(16)	118.58(18)	116.40(16)
N(1)−Ag(1)−P(1)	104.71(16)	103.22(18)	104.71(16)
N(1)−Ag(1)−P(2)	96.86(15)	96.68(16)	96.86(15)

Interestingly, the product of reaction 3 gave another complex **3b** when the crystallization was carried out in CH_2Cl/CH_3CN/ether. The products of the reactions 2 and 4 afforded crystals of complexes **2b** and **4** in CH_2Cl_2/ether and CH_2Cl_2/MeOH/ether, respectively.

Structures of Helical Polymers 1, 2a, and 3a. The X-ray crystal structures of $\{[Ag(\mu\text{-PAnP})(CH_3CN)(OTf)]\cdot 0.5CH_3CN\}_n$ (**1**), $\{[Ag(\mu\text{-PAnP})(CH_3CN)(ClO_4)]\}_n$ (**2a**), and $\{[Ag(\mu\text{-PAnP})(CH_3CN)(PF_6)]\}_n$ (**3a**) are shown in Figure 1, Figure S1 (Supporting Information), and Figure S2 (Supporting Information), respectively, and the selected bond lengths and angles are listed in Table 2.

The three complexes are polymeric, showing similar helical chains. Each helical chain is composed of PAnP which is coordinated to two Ag ions. The distances between adjacent Ag ions are ~8.2 Å. The two P−Ag vectors in the $[Ag_2(\mu\text{-PAnP})]$ unit show small torsional angles of ~10°. Part of the anthracenyl ring is "buried" in the interior of the helix, whereas the other end is exposed to the exterior. The phenyl rings of PAnP, the coordinated anions, and the acetonitrile protrude from the central axis of the helix. The pitches of the helices are 9.76, 9.70, and 9.76 Å for **1**, **2a**, and **3a**, respectively. While it has been shown that anions could affect the pitches in some Ag^I-helices of N-donor ligands,[4,15] they have virtually no effect on the Ag−PAnP polymers. The Ag^I ions in the three complexes are coordinated to two P atoms coming from two neighboring PAnP, the nitrogen atom of CH_3CN and the anion, showing a distorted trigonal pyramidal geometry. In each complex, the Ag^I atom is lifted slightly above the triangular plane defined by the P and N atoms by ~0.4 Å. The small distortion is caused by weak bonding interactions between the metal and the apical anions. The distances between the donor atoms

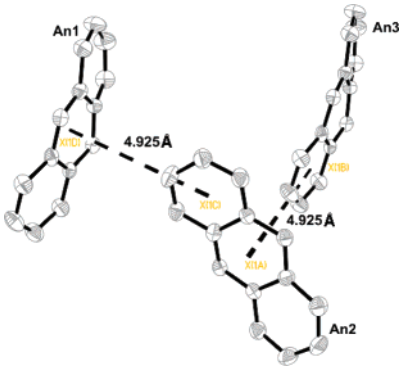

Figure 2. Diagram showing edge-to-face C−H···π interactions between three adjacent anthracenyl rings An1, An2, and An3 in **1**. X(1A) and X(1D) are the centroids of the central rings of An2 and An1, respectively, and X(1B) and X(1C) are centroids of lateral rings of An3 and An2, respectively. Thermal ellipsoids are drawn with 50% probability.

of the anions and the silver ions are long, being 2.519(5) (Ag−O), 2.679(2) (Ag−O), and 2.925(9) Å (Ag−F) for **1**, **2a**, and **3a**, respectively. The three complexes show similar P−Ag−P angles of ~150°. The torsional angles between the Ag−P bonds and the tetrahedral geometry of the metal ions and the phosphorus centers account for the "helicity" of the polymers.

Close inspection reveals intriguing edge-to-face C−H···π interactions between adjacent anthracenyl rings in a helix. As mentioned, part of the anthracenyl rings is embedded in the interior of the helical chain. As shown in Figure 2, two lateral ring protons in each anthracenyl ring are pointed to the central ring of its adjacent anthracenyl unit.

These interactions propagate along the central axis of the polymer with each anthracenyl ring acting as both hydrogen-bond donor and acceptor. The distances between the centriod (X1C) of the lateral ring and the centroid (X1D) of the central ring is 4.925 Å. Similar edge-to-face C−H···π interactions are also found in **2a** and **3a**. The two interacting rings are nearly perpendicular. These structural parameters fall within the range (4.5 Å < centroid-to-centroid distance < 7 Å) of aromatic C−H···π interactions.[13,16,17]

Structure of $[Ag_4(\mu\text{-PAnP})_4\supset(ClO_4)_2](ClO_4)_2\cdot 4CH_2Cl_2$ (2b). A macrocyclic $[Ag_4(\mu\text{-PAnP})_4\supset(ClO_4)_2](ClO_4)_2\cdot 4CH_2Cl_2$ **(2b)** was crystallized from CH_2Cl_2/diethyl ether mixture. The X-ray crystal structure of the cation $[Ag_4(\mu\text{-PAnP})_4\supset(ClO_4)_2]^{2+}$ reveals an intriguing tetrameric ring composed of four PAnP ligands and four Ag^I ions (Figure 3 and Table 3).

The four anthracenyl rings are nearly parallel to the central axis of the metallacycle, whereas the four metal ions are on the same plane. The complex exhibits a saddlelike structure with two opposite anthracenyl rings being positioned higher than the other pair. The torsional angle between two adjacent Ag−P bonds is 3.96°. In comparison to that of the helical

(15) Hirsch, K. A.; Wilson, S. R.; Moore, J. S. *Chem.—Eur. J.* **1997**, *3*, 765.

(16) Burley, S. K.; Petsko, G. A. *Science* **1985**, *229*, 23.

(17) (a) Bacon, G. E.; Curry, N. A.; Wilson, S. A. *Proc. R. Soc. London, Ser. A* **1964**, *279*, 98. (b) Kelbe, G.; Diederich, F. *Philos. Trans. R. Soc. London, Ser. A* **1993**, *345*, 37. (c) Oikawa, S.; Tsuda, M.; Kato, H.; Urabe, T. *Acta Crystallogr., Sect. B* **1985**, *41*, 437. (d) Bong, D. T.; Ghadiri, M. R. *Angew. Chem., Int. Ed.* **2001**, *40*, 2163. (e) Dance, I.; Scudder, M. *Chem.—Eur. J.* **1996**, *5*, 482.

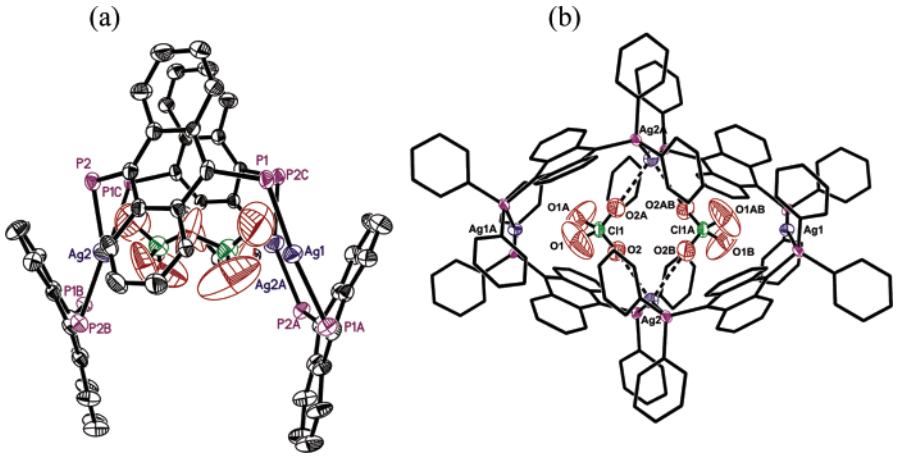

Figure 3. ORTEP plots of **2b** showing (a) the cation and two included ClO_4^- ions (Ph rings, solvent molecules, H atoms, and two anions are omitted) and (b) top view of the cation of **2b** (H atoms and two anions are omitted). Thermal ellipsoids are drawn with 50% probability.

Table 3. Selected Bond Lengths (Å) and Angles (deg) for Complexes **2b**, **3b**, and **4**

		2b	
Ag(1)−P(1)	2.4224(18)	P(1A)−Ag(1)−P(1)	168.20(9)
Ag(2)−P(2)	2.4416(19)	P(2B)−Ag(2)−P(2)	149.97(9)
Ag(1)−O(1)	3.014(18)		
Ag(2)−O(2)	2.783(9)		
		3b	
Ag(1)−N(1)	2.404(5)	P(1)−Ag(1)−P(2)	144.29(3)
Ag(1)−N(2)	2.432(5)	N(1)−Ag(1)−P(1)	96.28(11)
Ag(1)−P(1)	2.478(11)	N(2)−Ag(1)−P(1)	104.88(13)
Ag(1)−P(2)	2.4869(10)	N(1)−Ag(1)−N(2)	89.63(19)
Ag(2)−N(3)	2.413(6)	P(3)−Ag(2)−P(4)	142.79(4)
Ag(2)−N(4)	2.388(5)	N(3)−Ag(2)−P(3)	100.02(14)
Ag(2)−P(3)	2.4757(11)	N(4)−Ag(2)−P(3)	109.39(15)
Ag(2)−P(4)	2.4828(11)	N(3)−Ag(2)−N(4)	87.6(2)
		4	
Ag(1)−P(1)	2.401(2)	P(1)−Ag(1)−P(2)	167.04(10)
Ag(1)−P(2)	2.410(2)	P(2)−Ag(2)−P(3)	165.10(10)
Ag(3)−F(9A)	2.796(9)	P(6)−Ag(3)−P(5)	156.83(9)
		C(1)−P(1)−Ag(1)	109.2(3)

polymers, the Ag−Ag distance in **2b** is significantly shorter (6.903 Å). Intriguingly, two of the four ClO_4^- ions are encapsulated in the ring. The complex shows a D_2 symmetry with two C_2-axes, two pairs of opposite Ag ions Ag(1)−Ag(1A) and Ag(2)−Ag(2A), while the third C_2-axis passes through center of the ring. The encapsulated anions are close to the center of the ring with the two Cl atoms being separated by 4.673 Å. While the ClO_4^- ion has a T_d symmetry, the two ions form a dimeric unit of D_2 symmetry. That the metallacyle and the included anions share the same symmetry suggests that the formation of the ring is templated by the anions. As such, the complex represents a rare example where the formation of a metallacycle of low symmetry (D_2) is templated by a combination of two anions of high symmetry (T_d). The two pairs of perchlorate oxygen atoms, O(2) and O(2B) and O(2A) and O(2AB), are weakly coordinated (Ag−O = 2.786 Å) to Ag(2) and Ag(2A), respectively (Figure 3b). As a result of the interactions, the two silver ions exhibit a distorted tetrahedral geometry with the P−Ag−P units (P(2)−Ag(2)−P(2B) = 149.97(9)°). On the other hand, the coordination of the other two silver ions Ag(1) and Ag(1A) is almost linear.

Structure of $[Ag_2(\mu\text{-PAnP})_2(CH_3CN)_4](PF_6)_2\cdot 1.5Et_2O\cdot 0.35CH_2Cl_2$ (3b). Crystals of the binuclear complex $[Ag(\mu\text{-PAnP})(CH_3CN)_2]_2(PF_6)_2\cdot 1.5Et_2O\cdot 0.35CH_2Cl_2$ (**3b**) were isolated from a $Et_2O/CH_3CN/CH_2Cl_2$ mixture. X-ray analysis showed two independent molecules in the crystals whose structures are very similar, and accordingly, only one of them is discussed here. The cation of **3b** is a metallacycle composed of two PAnP linked by two Ag ions (Figure 4 and Table 3).

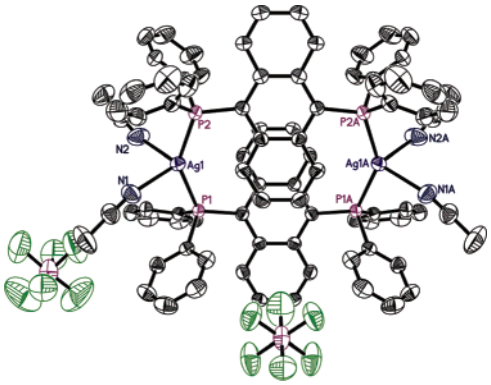

Figure 4. ORTEP plot of **3b**. Thermal ellipsoids are drawn with 50% probability. Solvent molecules and hydrogen atoms are omitted for clarity.

The complex displays C_{2h} symmetry with the C_2-axis passing through the two Ag ions. The two anthracenyl rings are parallel and partially overlapped. The shortest distance between the rings is 4.33 Å. The two Ag ions are widely separated by 8.041 Å, and both $[Ag_2(\mu\text{-PAnP})]$ units are in syn conformation. Apart from the P atoms of PAnP, each Ag ion is bonded to two CH_3CN molecules, showing a distorted tetrahedral geometry. Notably, the PF_6^- ions do not coordinate to the metal ions. The Ag−P (2.4757(1)−2.4869(1) Å) and Ag−N bond (2.388(5)−2.432(5) Å) distances are similar to the corresponding parameters found in the polymeric complexes.

Structure of $[Ag_3(\mu\text{-PAnP})_3\supset BF_4](BF_4)_2\cdot 4Et_2O\cdot CH_3OH$ (4). Crystals of $[Ag_3(\mu\text{-PAnP})_3\supset BF_4](BF_4)_2\cdot 4Et_2O\cdot CH_3OH$ (**4**) were obtained from a CH_2Cl_2/diethyl ether mixture. X-ray analysis shows that the cation of $[Ag_3(\mu\text{-PAnP})_3\supset BF_4](BF_4)_2\cdot 4Et_2O\cdot CH_3OH$ is a trinculear ring composed of three bridging PAnP ligands and three Ag ions (Figure 5 and Table 3).

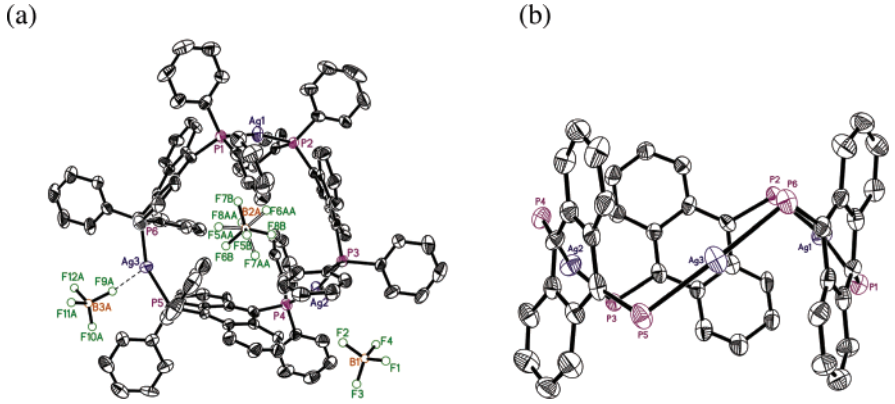

Figure 5. ORTEP plots of the cation of **4** showing (a) the top view and (b) side view of the molecule. Thermal ellipsoids are drawn with 50% probability. Solvent molecules, H atoms, phenyl rings, and anions (for the side view) are omitted for clarity.

Table 4. $^{31}P\{^1H\}$-NMR Data of Complex **1**, **2a**, **2b**, **3a**, **3b**, and **4**

	CD_3CN δ (J^{107}_{Ag-P}, J^{109}_{Ag-P}/Hz)		CD_2Cl_2 δ (J^{107}_{Ag-P}, J^{109}_{Ag-P}/Hz)	
complexes	300 K[a]	238 K	300 K	193 K
complex **1**	3.26	4.52 (458, 515) 1.43 (438, 500)		
complex **2a**	3.20	4.53 (454, 523) 1.24 (431, 504)		
complex **3a**	3.23	4.55 (454, 526) 1.19 (435, 504)		
complex **2b**	3.20	4.50 (453, 522) 1.35 (431, 496)	3.72 (515, 599)	7.01 (443, 523), 3.39 (530, 610), 2.45 (477, 557), 0.89 (504, 584), 0.25 (522, 603)
complex **3b**	3.23	4.50 (453, 520) 1.23 (434, 501)	5.13 (526, 607)	four double doublet signals in δ −3.72 to 9.51
complex **4**	2.48	4.42 (454, 519) 1.19 (435, 500)	4.02 (522, 603)	two broad signals at δ 3.0 and 0.3

[a] All signals are broad and show no J_{Ag-P} coupling.

The metallacycle shows a puckered conformation similar to the chair conformation of cyclohexane (Figure 5b). Similar structure was observed in the gold ring $[Au_3(\mu\text{-PAnP})_3)\supset ClO_4]$-$(ClO_4)_2$.[11] Unlike the other Ag−PAnP complexes, the Ag−P bonds show a large dihedral angle of 102°. The three anthracenyl rings are nearly parallel to the central axis of the ring, and the distance between P1 and P4 is 9.897 Å. One of the BF_4^- ions is included in the middle of the ring and is disordered over two positions. Another BF_4^- ion is weakly bonded to one of the Ag ions, showing a long Ag−F distance of 2.79 Å.[8c] Because of the bonding interactions, the silver ion displays a distorted trigonal planar geometry, showing a P−Ag−P angle (P(5)−Ag(3)−P(6) = 156.83-(9)°) significantly smaller than the other two Ag ions in the complex (167.04(10)° and 165.10(10)°). Analogous to the diatopic axial and equatorial H atoms of cyclohexane, the silver ring has six axial phenyl rings lying up and down along the central axis of the ring and six equatorial phenyl rings alternating about a plane at right angles to the central axis.

VT $^{31}P\{^1H\}$-NMR in CD_3CN. The existence of an equilibrium of different Ag−PAnP complexes in solution was first suggested by the fact that different products were isolated by changing the crystallization solvents and was further verified by a VT $^{31}P\{^1H\}$-NMR study. Despite their different structures, room-temperature spectra of the polymeric and macrocyclic complexes measured in CD_3CN are surprisingly similar. The spectra of polymeric **1** and macrocyclic **2b** are shown in parts a and b of Figure 6, respectively (see Figures S3−S6 for the spectra of **2a**, **3a**, **3b**, and **4**). The spectroscopic data are summarized in Table 4.

All spectra show a broad signal at ~δ 3 with no $J^{107/109}_{Ag-P}$ coupling. Unlike the broad ^{31}P NMR signals, the ^1H NMR spectra are well resolved. This indicates that the dynamics involve dissociation and formation of the Ag−P bond, the rate of which should be comparable to the NMR time scale.[8e] The temperature dependence of all of the spectra is similar: lowering the temperature to 278 K leads to the appearance of two broad peaks which are resolved at 238 K into two double doublets at δ 4.42−4.55 (low field) and δ 1.19−1.43 (high field). Both sets of signals display J_{Ag-P} coupling. Notably, the signals of all the spectra show similar chemical shifts and coupling constants (Table 4). For **1**, **2a**,**b**, and **3a**,**b**, the low-field signals (δ 4.50−4.55) are weaker than the high-field signals (δ 1.19−1.43), but the low-field signal (δ 4.42) in the spectrum of **4** is more intense than the high-field one (δ 1.19).

Variable-Temperature $^{31}P\{^1H\}$ NMR in CD_2Cl_2. Because of the insolubility of the polymeric **1**, **2a**, and **3a** in CD_2Cl_2, only the VT ^{31}P NMR spectra of **2b**, **3b**, and **4** in that solvent were studied. The room-temperature ^{31}P NMR spectra of the three complexes (Figure 7 for **2b** and Figures S7 and S8 for **3b** and **4**, respectively) are drastically different from the corresponding ones recorded in CD_3CN.

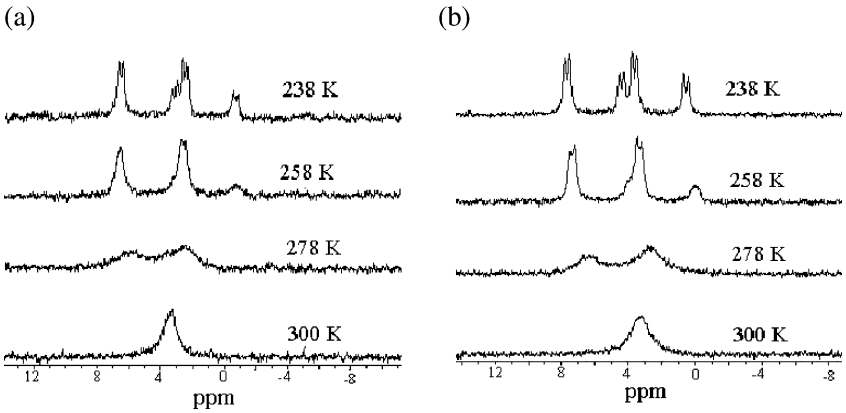

Figure 6. VT $^{31}P\{^1H\}$-NMR spectra of (a) **1** and (b) **2b** measured in CD_3CN.

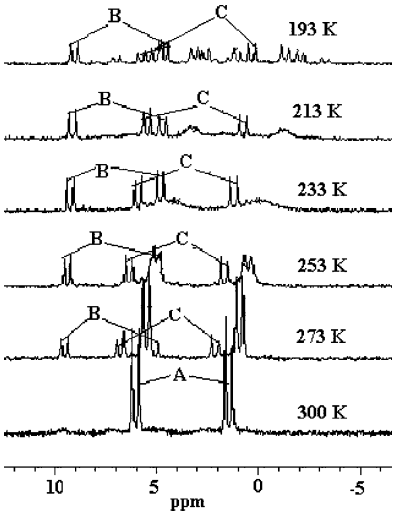

Figure 7. VT $^{31}P\{^1H\}$-NMR spectra of **2b** recorded in CD_2Cl_2.

Unlike the spectra measured in CD_3CN, the room-temperature spectra of **2b**, **3b**, and **4** in CD_2Cl_2 all exhibit a sharp double doublet with J_{Ag-P} couplings. While the chemical shifts of the signals are different, being δ 3.72, 5.13, and 4.02 for **2b**, **3b**, and **4**, respectively, their J_{Ag-P} constants are rather similar (J^{109}_{Ag-P} = 599−603 Hz and J^{107}_{Ag-P} = 515−522 Hz).

The temperature-dependent behaviors of the spectra of the CD_2Cl_2 are more complicated than the ones in CD_3CN. In addition to the intense double doublet (Figure 7, signal A) at δ 3.72 (J^{107}_{Ag-P} = 515 Hz, J^{109}_{Ag-P} = 599 Hz), the room-temperature spectrum of **2b** shows some weak and broad signals which resolve at 273 K into two double doublets (Figure 7, signals B and C) at δ 7.28 (J^{107}_{Ag-P} = 496 Hz, J^{109}_{Ag-P} = 572 Hz) and 5.65 (J^{107}_{Ag-P} = 465 Hz, J^{109}_{Ag-P} = 595 Hz), respectively. However, the appearance of the signals B and C does not affect the intensity of signal A, suggesting that the signals could come from small amounts of unknown Ag−PAnP complexes crystallized along with **2b**. At 193 K, the broad signal derived from signal A is resolved into three double doublets at δ 3.39 (J^{107}_{Ag-P} = 530 Hz, J^{109}_{Ag-P} = 610 Hz), 0.89 (J^{107}_{Ag-P} = 504 Hz, J^{109}_{Ag-P} = 584 Hz), and 0.25 (J^{107}_{Ag-P} = 522 Hz, J^{109}_{Ag-P} = 603 Hz). Similarly, the double doublet in the room-temperature spectrum of **3b** is broadened as temperature decreases, and several doublets are found between δ −3.72 and 9.51 at 193 K (Figure S7). The sharp double doublet of **4** becomes two broad peaks at δ 3.0 and 0.3 as the temperature is lowered from 300 to 233 K (Figure S8). Four broad signals are observed when the sample is cooled to 193 K.

Proposed Dynamics. The VT NMR study shows that the solution dynamics of the complexes are solvent-dependent with the exchange in CD_3CN being "simpler" than the ones in CD_2Cl_2. Despite their different structures, the ESI-MS of **1**, **2a**,**b**, **3a**,**b**, and **4** (Figures S9, S10, S12, and S14) are similar, showing peaks ascribable to $[Ag(PAnP)]_n^{n+}$ (*m*/z 654.3), $[Ag_2(PAnP)_3]^{2+}$ (*m*/z 926.9), $[Ag(PAnP)_2]^+$ (*m*/z 1201.0), and $[Ag(PAnP)_3]^+$(*m*/z 1745.4). The molecular ions could arise from fragmentation of the helical polymer and/or oligomers (cyclic or linear). Although no peak assignable to the metallacycles **2b**, **3b**, and **4** are found, the existence of the complexes could not be ruled out as the rings could have low ionizability or poor stability under the conditions of ESI-MS measurements.

Interestingly, all the ^{31}P NMR spectra recorded in CD_3CN show similar signals and temperature-dependent behavior; regardless of their different structures (discrete metallacycles or polymers), all the spectra recorded in CD_3CN display a broad peak at room temperature which is resolved into two double doublets at low temperature. As the dynamics involve dissociation of the Ag−P bond, it is unlikely that the two signals are due to different conformations of a complex. Rather, the results are more consistent with an exchange involving two different species. Furthermore, as all of the complexes show similar signals at low temperature, it is likely that the complexes convert to the same two species when they are dissolved in acetonitrile. In other words, the two species must be attainable from all of the silver complexes, and they should be more stable than other possible structures in acetonitrile. It is therefore possible that one of them is the helical polymer $[Ag(\mu\text{-PAnP})(CH_3CN)X]_n$ (X = OTf, ClO_4, BF_4, or PF_6) as the helices were universally obtained from acetonitrile solutions of the products of all the reactions. The other complex could be the dimeric $[Ag_2(\mu\text{-PAnP})_2(CH_3CN)_2]^{2+}$, the cation of **3b**. The reason is that of all the silver metallacycles isolated, the dimer is the only one that does not have an encapsulated anion. It suggests that the formation of the dimer is independent of the anion.

Scheme 2

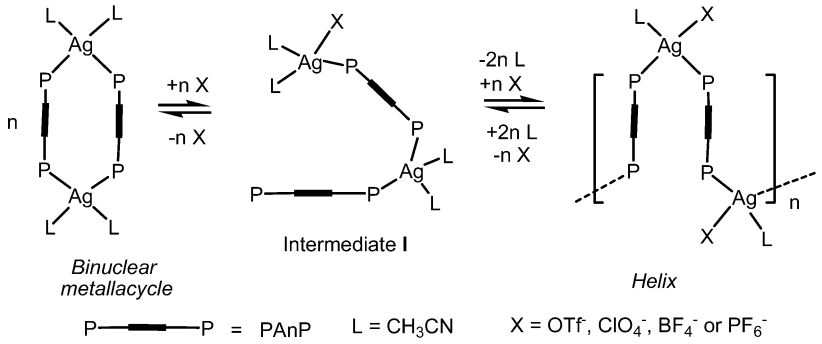

Furthermore, the dimer and the helix could be stabilized by the coordination of CH_3CN.

A reversible ring-opening polymerization of the binuclear complex is proposed to be the exchange mechanism. Ring-opening polymerization was invoked to explain generation of polymeric structures from gold(I)-phosphine,[7b,18] silver-(I)-phosphine, and silver metallacycles.[8] In the first step of the proposed mechanism (Scheme 2), a Ag−P bond in $[Ag_2(\mu\text{-PAnP})_2(CH_3CN)_2]^{2+}$ dissociates to form an intermediate **I**, which has a Ag ion and a free phosphorus atom at its head and tail positions.

The bond cleavage could be facilitated by coordination of the anion or solvent. Head-to-tail polymerization of the intermediate **I** leads to the helix. The free energy of the intermediate **I** could be significantly higher in energy than that of the binuclear complex and the helix as only the signals of the two species are observed at 238 K.

Exchange processes in CD_2Cl_2 solutions of **2b**, **3b**, and **4** are complicated. The solutions of the three complexes show different temperature-dependent behaviors, and more than two species are involved in the exchange. The ESI-MS of the complexes recorded in CH_2Cl_2 are similar to the ones in CH_3CN. All three complexes show a sharp double doublet signal at room temperature, suggesting that either the Ag−P dissociation and formation are faster than the NMR time scale or the two processes occur concomitantly. It is reasonable because dichloromethane, being a very weak ligand, is unable to stabilize intermediates arising from Ag−P cleavage.

Luminescence. All of the silver complexes display intense solid-state emission. The fluorescence spectra are shown in Figure 8.

All emissions show two vibronic peaks at 488 and 530 nm. It is believed that the luminescence arises from a $\pi\pi^*$ excited-state localized in the anthracenyl ring of the ligand PAnP. It is supported by the fact that emissions of similar energy were observed in spectra of other PAnP-containing complexes such as $[Au_3(\mu\text{-PAnP})_3\supset ClO_4](ClO_4)_2$[11] and $[Au_4(\mu\text{-PAnP})_2(4,4'\text{-bipyridine})_2](OTf)_4$.[12]

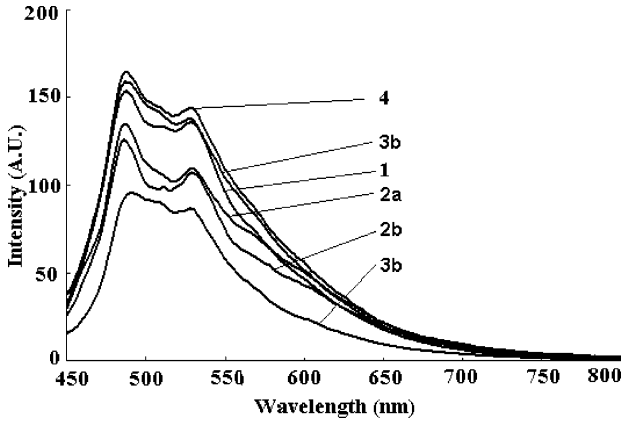

Figure 8. Room-temperature solid-state emission spectra of **1**−**4**.

Concluding Remarks. In this work we have demonstrated the rich structural diversity of Ag−PAnP compounds arising from the equilibrium of different complexes in solutions. The structures obtained are dependent on the solvent used for crystallization and the anion. Helical polymers are obtained from CH_3CN, whereas discrete metallacycles of different nuclearity are crystallized from CH_2Cl_2 or mixtures of CH_2Cl_2 and CH_3CN. VT NMR spectroscopy shows that the solution dynamics and distribution of the silver complexes are influenced by the solvent. The mechanism of the exchange in CD_3CN is believed to be a ring-opening polymerization of the dinuclear metallacycle. On the other hand, the dynamic processes in CD_2Cl_2 are far more complicated, involving more than two exchanging species.

Acknowledgment. The authors thank National University of Singapore for financial support and Ms. Tan Geok Kheng and Professor Koh Lip Lin for assistance with the X-ray crystal structure determination.

Supporting Information Available: Crytallographic data in CIF format, synthetic procedures and characterizations of the complexes, crystal structures of **2a** and **3a**, and ESI-MS and VT $^{31}P\{^1H\}$-NMR spectra of **2a**, **3a**, **3b**, and **4** in CD_3CN and **3b** and **4** in CD_2Cl_2. This material is available free of charge via the Internet at http://pubs.acs.org.

IC060140V

(18) (a) Burchell, T. J.; Eisler, D. J.; Jennings, M. C.; Puddephatt, R. J. *J. Chem. Soc., Chem. Commun.* **2003**, 2228. (b) Puddephatt, R. J. *Macromol. Symp.* **2003**, *196*, 137. (c) Qin, Z. Q.; Jennings, M. C.; Puddephatt, R. J. *Chem.—Eur. J.* **2002**, *8*, 735.